NUCL SCI TECH (2019) 30:113
https://doi.org/10.1007/s41365-019-0627-x

Simulation study of longitudinal injection scheme for HALS with a higher harmonic cavity system

Zhen-Biao Sun[1] · Lei Shang[1] · Feng-Lei Shang[1] · Yun-Gai Tang[1] · Wei Liu[1] · Wen-Bin Song[1]

Received: 25 September 2018 / Revised: 25 February 2019 / Accepted: 10 March 2019 / Published online: 12 June 2019

Abstract Longitudinal injection is a promising on-axis injection scheme for diffraction-limited storage rings. In the latest version of the Hefei advanced light source (HALS), both the dynamic aperture and momentum aperture have been optimized. A longitudinal injection scheme was investigated on the HALS using a double-frequency radio frequency system. To evaluate the injection performance, various errors were considered. A series of tracking simulations were conducted, and the injection efficiency was obtained under different error levels.

Keywords Longitudinal injection · Hefei advanced light source · Double-frequency RF system · Injection efficiency

1 Introduction

The Hefei advanced light source (HALS) is a newly designed high-performance DLSR-based light source proposed by the National Synchrotron Radiation Laboratory (NSRL) in China. After several optimizations, the dynamic aperture (DA) and momentum aperture (MA) of HALS were enlarged [1, 2], but the DA in the horizontal plane is still only approximately 2 mm. Considering that the machine aperture of HALS is 10 mm, on-axis injection seems a promising scheme for beam injection for the HALS.

There are two types of on-axis injection that have been proposed: swap-out injection [3] and longitudinal injection [4]. Swap-out injection uses an accumulation ring for beam accumulation, and the accumulation ring is almost the same size as the main storage ring, so the construction costs will increase. Another way to adopt swap-out injection is to use a linac or booster directly as an injector, but weakened beams from the storage ring must be discarded, and the radiation level would increase. Longitudinal injection is another on-axis injection scheme proposed by the Swiss Light Source (SLS) [5]. It uses short-pulse kickers to kick an injecting bunch transversely on-axis between two circulating bunches. It is an effective and much simpler scheme without significant changes of the hardware of the storage ring.

Longitudinal injection has strict requirements on energy acceptance and more technical challenges for fast kickers. Some new injection schemes have been proposed based on longitudinal injection. The Shanghai Synchrotron Radiation Facility (SSRF) attempted to use fundamental and second-harmonic cavities for longitudinal injection with bunch merging [6–8]. The on-axis beam accumulation scheme of the high energy photon source (HEPS) is based on a triple-frequency radio frequency (RF) system [9]. Longitudinal injection with "longitudinal nonlinear kicker" is applied to the upgrade of the French light source SOLEIL to improve the capture of the high-momentum beam [10].

The MA of the HALS is large enough for longitudinal injection. In this work, the goal is to verify the feasibility of the longitudinal injection method on the HALS. To be close to the actual situation, a higher harmonic cavity

This work was supported by the National Key R&D Program of China (No. 2016YFA0402002).

✉ Lei Shang
lshang@ustc.edu.cn

[1] National Synchrotron Radiation Laboratory, University of Science and Technology of China, Hefei 230029, China

(HHC) system is included in this study. In Sect. 2, a brief introduction to the HALS is provided, and a double-frequency RF system is discussed. To simulate a realistic machine, various errors were introduced, and accelerator simulation program elegant was used for particle tracking, as described in Sect. 3.

2 Injection system of the HALS

2.1 Longitudinal injection

The HALS is a vacuum ultraviolet (VUV) and soft-X ray light source with an energy of 2.4 GeV and a circumference of 672 m. In the latest version of the HALS lattice design, longitudinal gradient bends and antibends are employed, and a lower natural emittance of 23.2 pm rad is achieved. Meanwhile, the nonlinear dynamics for this version of the lattice is improved. The main parameters of the latest design of the HALS are listed in Table 1.

To keep the circulating bunches undisturbed, the pulse of the kicker field has to be shorter than the bunch spacing. The main RF frequency f_{rf} was chosen as 100 MHz to reduce the technical difficulties of the kickers. The synchronous phase φ_0 and momentum acceptance δ_{acc} are given by:

$$\varphi_0 = \pi - \arcsin\left(\frac{U_0}{eV_{\mathrm{rf}}}\right), \tag{1}$$

$$\delta_{\mathrm{acc}} = \sqrt{-\frac{2eV_{\mathrm{rf}}}{\pi h\alpha E_0}\left[\cos(\varphi_0) + \left(\varphi_0 - \frac{\pi}{2}\right)\sin(\varphi_0)\right]}, \tag{2}$$

where U_0 is the energy loss per turn caused by synchrotron radiation, V_{rf} is the RF voltage, h is the harmonic number, and α is the momentum compaction factor. The momentum compaction factor of the HALS is 3.5×10^{-5}. The bucket height is 5.15% without considering the synchrotron radiation effect, when the RF voltage is set as 350 kV. Figure 1 shows the longitudinal phase space of the HALS. The red lines indicate the border of the stable bucket, the gray lines indicate trajectories outside the acceptance, and the cyan lines show the particle trajectories that have been tracked for 65,000 turns in the longitudinal phase space with synchrotron radiation loss.

Table 1 Main parameters of the HALS

Parameter	Value
Beam energy (GeV)	2.4
Circumference (m)	672
Natural emittance (pm rad)	23.2
Radiation loss (keV/turn)	217.6
Harmonic number	224
Momentum compaction factor	3.5×10^{-5}
Tune, ν_x/ν_y	78.33/29.30
Damping time, $\tau_x/\tau_y/\tau_s$ (ms)	32.7/49.4/33.2
Natural chromaticities	− 109/− 126

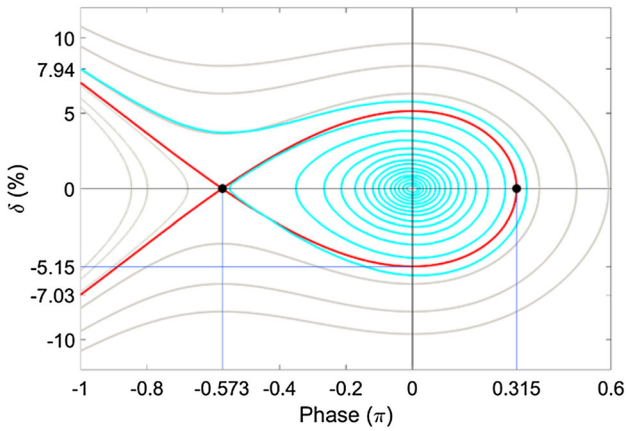

Fig. 1 (Color online) Longitudinal phase space of the HALS

The bunch spacing is 10 ns when a 100-MHz fundamental RF cavity is adopted. If a bunch is injected with a time offset of − 5 ns with respect to the circulating bunch, its upper limit and lower limit of momentum offset are 7.94% and 7.03%, respectively. Particles with higher or lower momentum offset would be lost. Particles in the stable bucket would merge to the circulating bunches because of radiation damping in the longitudinal phase space. This process takes four to five times of the longitudinal damping time; the higher energy the particle has, the shorter the time it requires.

2.2 Double-frequency RF system

In a storage ring, an HHC is necessary to reduce the Touschek scattering and, thus, improve the beam lifetime. In addition, the longitudinal acceptance can be enlarged with an HHC. Both a second-harmonic cavity (2HC) and a third harmonic cavity (3HC) are taken into consideration. For a passive HHC, the induced voltage is [11]

$$V_{\mathrm{h}}(\tau) = A\cos\varphi_{\mathrm{h}}\cos(n\omega_{\mathrm{rf}}\tau - \varphi_{\mathrm{h}}), \tag{3}$$

where the longitudinal coordinate τ is the time distance from the synchronous particle, A is a factor, φ_{h} is the tuning angle of the HHC, n is the harmonic cavity number, and $\omega_{\mathrm{rf}} = 2\pi f_{\mathrm{rf}}$ is the resonant frequency of the main RF. The total voltage is then [12]

$$V_{\mathrm{t}}(\tau) = V_{\mathrm{rf}}\sin(\omega_{\mathrm{rf}}\tau + \varphi_{\mathrm{s}}) + A\cos\varphi_{\mathrm{h}}\cos(n\omega_{\mathrm{rf}}\tau - \varphi_{\mathrm{h}}). \tag{4}$$

When an HHC is included, the synchronous phase of the main RF changes, and it is expressed by φ_{s}. The optimal

bunch lengthening condition of the passive HHC is given by [13–15]

$$\varphi_h = -\arccos\sqrt{\frac{U_0}{eA(1-n^2)}},$$
$$\varphi_s = \pi - \arcsin\left[\frac{U_0 n^2}{eV_{rf}(n^2-1)}\right], \quad (5)$$
$$A = \frac{(1-n^2)V_{rf}^2 + n^2\left(\frac{U_0}{e}\right)^2}{n^2\left(\frac{U_0}{e}\right)}.$$

The potential of a passive HHC is

$$\Phi(\tau) = \frac{\alpha e}{E_0 T_0 \omega_{rf}} \left\{V_{rf}[\cos\varphi_s - \cos(\omega_{rf}\tau + \varphi_s)] + \frac{A\cos\varphi_h}{n}[\sin\varphi_h + \sin(n\omega_{rf}\tau - \varphi_h)]\right\} - \frac{\alpha U_0 \tau}{E_0 T_0}. \quad (6)$$

Two types of double-frequency RF system were investigated: a main RF with a 2HC and main RF with a 3HC. Detailed parameters of these two RF systems are listed in Table 2. The harmonic number is 224; then, the bunch spacing of two stored bunches is 10 ns, or 3 m. Figure 2 shows waveforms of cavity voltages and potential function with and without an HHC when n is 2 or 3. The green solid ellipse in the figure indicates the stored bunch. As can be seen in Fig. 2b, the potential function is obviously flattened when an HHC is attached.

As for the parameters of Table 1, elegant [16] is used for particle tracking. The longitudinal acceptances of the HALS with and without an HHC are depicted in Fig. 3. When radiation damping in longitudinal phase space is taken into account, the bucket height of an RF system with a 3HC is approximately 5.8%, the same as that of an RF system without an HHC. The bucket height of an RF system with a 2HC reduces to 4%. The energy offset is approximately 8% when the bunch is injected at − 5 ns. Although the MA at a long straight section may achieve 8%, one must consider the off-momentum DA for a better injection efficiency, because the injection bunches have an energy offset in a longitudinal injection scheme. Figure 4 shows that the off-momentum DA is small when a bunch is injected with a momentum offset of 8%, and the DA is larger when the momentum offset is less than 6%. In addition, the smaller the time offset is, the larger the energy and phase acceptance are. The longitudinal acceptance of a 3HC system is larger, but it does not perform better in injection simulations than the 2HC system. Although the 3HC system has a higher bucket height, its off-momentum DA is smaller than that of the 2HC system. After repeated simulations, (dt, δ) = (3.6 ns, 3.2%) was chosen as the injection point for the 2HC case. The corresponding energy and phase acceptance are approximately 0.85% and

Table 2 Parameters of double-frequency RF system

Type of HHC	V_{rf} (kV)	φ_s (°)	V_h(kV)	φ_h (°)
Main RF + 2HC	350	124.01	− 121.83	− 53.46
Main RF + 3HC	350	135.62	− 87.67	− 71.93

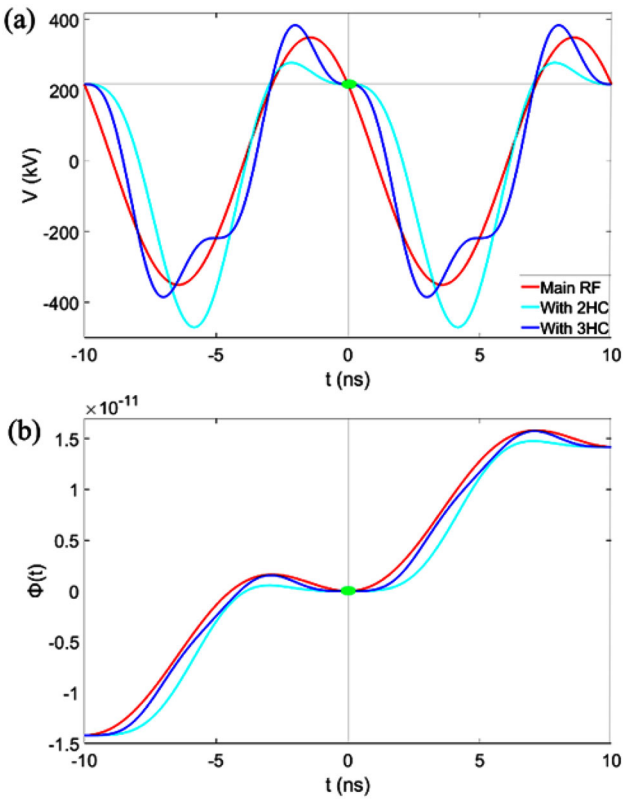

Fig. 2 (Color online) **a** Waveforms of RF voltage. **b** Waveforms of potential function

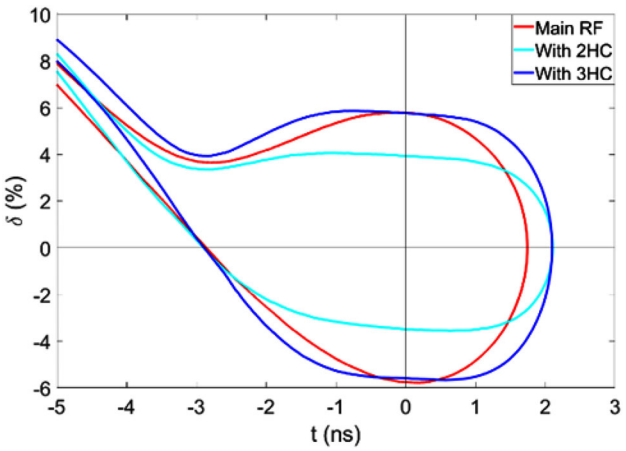

Fig. 3 (Color online) Longitudinal acceptance of the HALS

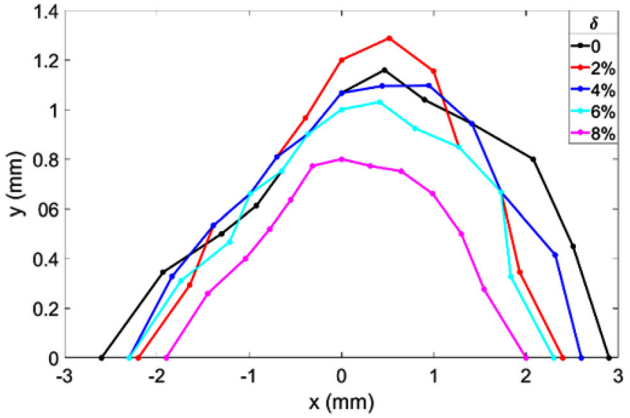

Fig. 4 (Color online) Off-momentum DA of the HALS

0.14 rad (190 ps), respectively—sufficient to tolerate jitters from the injection beam.

3 Results and discussion

3.1 Error analysis

In a realistic machine, various errors may occur. This study classifies errors from the entire injection process into three types: beam mismatch error, beam trajectory error, and misalignment error [17, 18]. The beam mismatch error comes from errors of the injector and transport line, leading to mismatched injected bunches with unexpected beam energy, emittance, energy spread, and bunch length. The injector of the HALS is a full energy linac. The design requirements for injected bunches are a normalized emittance of 2 mm mrad, a bunch length of approximately 10 ps (FWHM), and an energy spread less than 0.1%. To simulate beam mismatch error, the injected bunch is assumed to have an emittance of 2.0 nm rad, an energy spread of 0.1%, and 20 ps rms bunch length.

Beam trajectory error resulted from errors of the injection system, including trajectory error at the injection point, pulse-to-pulse jitter, and bending angle errors of the septum and strip-line kickers. The beam trajectory error was equivalent to deviations of (x, x', y, y') of the injected bunches, a four-dimensional error. First, for the convenience of simulation, the impact of errors in each single dimension on the capture efficiency of injected bunches was analyzed. The variation trends of capture efficiency under respective deviation of x, x', y, and y' are shown in Fig. 5. Figure 5 shows that the HALS has less tolerance to the deviations of y and x'. Table 3 summarizes the ranges of respective deviations when the capture efficiency is more than 80%. These four types of deviation have no correlations with each other. Their correlations are shown in the next section.

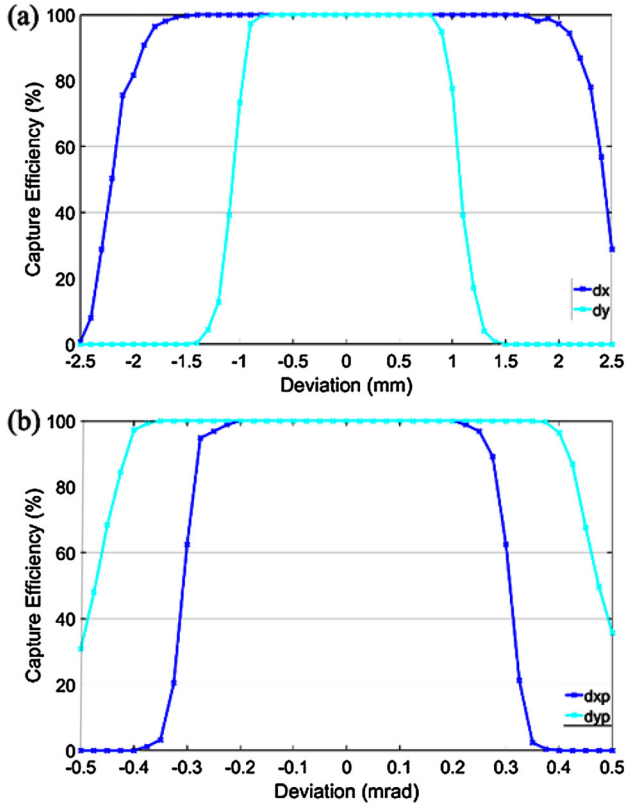

Fig. 5 (Color online) **a** Capture efficiency under deviations of x and y. **b** Capture efficiency under deviations of x' and y'

Table 3 Deviation ranges of the injected beam

Deviation variable	Range of > 80% efficiency
Δx (mm)	[− 2.03, 2.28]
$\Delta x'$ (mrad)	[− 0.29, 0.28]
Δy (mm)	[− 0.97, 0.98]
$\Delta y'$ (mrad)	[− 0.43, 0.44]

3.2 Error analysis and simulation study

To investigate how the longitudinal injection scheme performs on the HALS, both beam mismatch error and beam trajectory error were then introduced to simulate a realistic machine. The parameters of beam mismatch error are presented in Sect. 3.1. The beam trajectory error was equivalent to a four-dimensional variable $(\Delta x, \Delta y, \Delta x', \Delta y')$. The injected beam was set as $\Delta x = -0.2$ mm, $\Delta y = -0.1$ mm, $\Delta x' = -0.06$ mrad, and $\Delta y' = -0.06$ mrad. A bunch of 1000 particles was tracked for 60,000 turns. The simulation results are shown in Fig. 6. Figure 6a is the distribution of particles in the longitudinal plane, and Fig. 6b, c show the particles in transverse phase space. After 60,000 turns, the injected

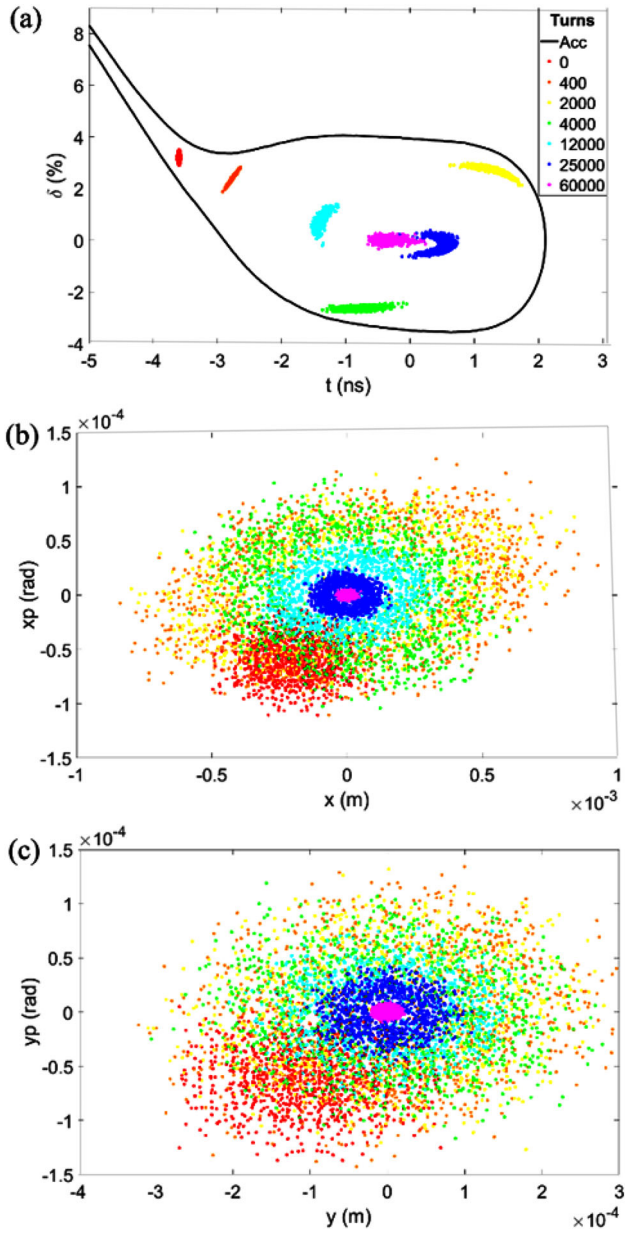

Fig. 6 (Color online) Particle distributions in the longitudinal and transverse planes

bunch was successfully damped, and no particle was lost in the simulation. This means longitudinal injection performs well on the HALS when beam mismatch error and beam trajectory error are introduced.

To get closer to the realistic machine condition, errors of misalignments were then introduced. One hundred random errors were assigned to the quadrupole and sextupole magnets: quadrupole and sextupole roll errors of 0.2 mrad, quadrupole and sextupole fractional magnet strength of 5×10^{-4}, and transverse sextupole misalignments of 20 μm. In this simulation, the beam mismatch error was the same as Sect. 3.1, and the beam trajectory error was at a

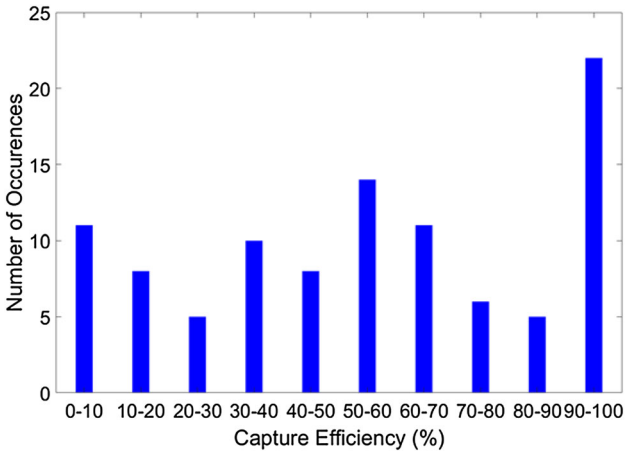

Fig. 7 Distribution of capture efficiency over misalignments

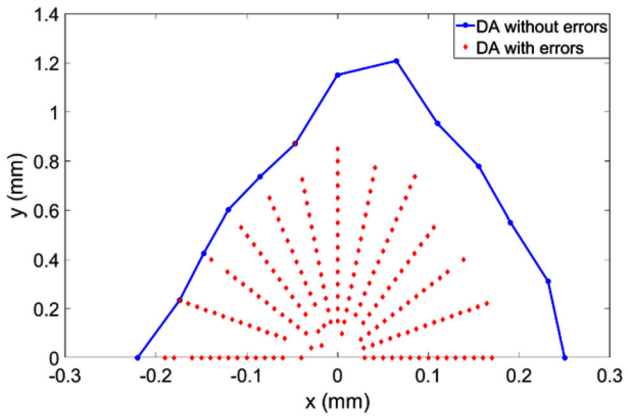

Fig. 8 DA of the HALS with and without misalignments

lower level: $\Delta x = -0.05$ mm, $\Delta y = -0.05$ mm, $\Delta x' = -0.05$ mrad, and $\Delta y' = -0.05$ mrad. One thousand particles with a Gaussian distribution were tracked for 3600 turns for 100 random cases. As a result of the simulation, 100 groups of data were generated. Figure 7 shows a bar chart of the capture efficiency distribution over 100 random errors. The abscissa indicates ranges of capture efficiency, and the ordinate indicates the number of occurrences corresponding to capture efficiency. The performance was poor with misalignments; only 27 of 100 random seeds gave an efficiency of more than 80%. The small DA of the HALS was thought to be the problem, so the DA was tracked for another 100 random cases with misalignments, and 100 groups of DA data were generated. The blue line in Fig. 8 is the DA without misalignments, and the red point is the DA of 100 seeds with misalignments. The minimum DA with misalignments was almost 0. The lattice needs to be further optimized for a larger DA to adopt longitudinal injection scheme for the HALS.

4 Conclusion

Longitudinal injection is a promising on-axis scheme for the beam injection of DLSRs. The latest version of the HALS has some advantages for longitudinal injection scheme, such as a higher bucket height of 6% and a dynamic MA of 8%. However, the dynamic aperture of the HALS is only approximately 2 mm, and this may add additional difficulties for beam injection. A 2HC system was used, and a lower energy offset was chosen to improve tolerance for errors. In the simulations, many types of error were analyzed that may occur in a realistic injection progress. The system performed well with mismatch error and injected beam trajectory error. However, when misalignment errors were introduced, there was a serious particle loss. For a better injection efficiency, the HALS lattice needs further optimization.

References

1. Z.H. Bai, W. Li, L. Wang, et al., Design study for the first version of the HALS lattice, in *Proceedings of IPAC2017, Copenhagen, Denmark* (2017), pp. 2713–2715. https://doi.org/10.18429/jacow-ipac2017-wepab060
2. Z.H. Bai, W. Li, L. Wang, et al., Design of the second version of the HALS storage ring lattice, in *Proceedings of IPAC2018, Vancouver, BC, Canada* (2018), pp. 4601–4604. https://doi.org/10.18429/jacow-ipac2018-thpmk121
3. L. Emery, M. Borland, Possible long-term improvements to the advanced photon source, in *Proceedings of the 2003 Particle Accelerator Conference* (2003), pp. 256–258. https://doi.org/10.1109/pac.2003.1288895
4. M. Aiba, M. Böge, F. Marcellini et al., Longitudinal injection scheme using short pulse kicker for small aperture electron storage rings. Phys. Rev. Spec. Top. Accel. Beams **18**(2), 020701 (2015). https://doi.org/10.1103/PhysRevSTAB.18.020701
5. A.S. Hernández, M. Aiba, Investigation of the injection scheme for SLS 2.0, in *Proceedings of IPAC2015, Richmond, VA, USA* (2015), pp. 1720–1723. https://doi.org/10.18429/jacow-ipac2015-tupje046
6. B.C. Jiang, Z.T. Zhao, S.Q. Tian et al., Using a double-frequency RF system to facilitate on-axis beam accumulation in a storage ring. Nucl. Instrum. Methods Phys. Res. Sect. A **814**, 1–5 (2016). https://doi.org/10.1016/j.nima.2016.01.024
7. B.C. Jiang, G.Q. Lin, B.L. Wang et al., Multi-bunch injection for SSRF storage ring. Nucl. Sci. Tech. **26**, 050101 (2015). https://doi.org/10.13538/j.1001-8042/nst.26.050101
8. S.Q. Tian, Q.L. Zhang, M.Z. Zhang et al., Low emittance lattice design with Robinson wiggler in the arc section. Nucl. Sci. Tech. **28**, 9 (2017). https://doi.org/10.1007/s41365-016-0166-7
9. G. Xu, J. Qiu, Z. Duan, et al., On-axis beam accumulation enabled by phase adjustment of a double-frequency rf system for diffraction-limited storage rings, in *Proceedings of IPAC2016, Busan, Korea*. 2013–2025 (2016). https://doi.org/10.18429/jacow-ipac2016-weoaa02
10. M.A. Tordeux, Longitudinal injection into low-emittance ring: a novel scheme for SOLEIL upgrade, in *Topical Workshop on Injection and Injection System*. https://indico.cern.ch/event/635514/contributions/2660490/
11. M. Migliorati, L. Palumbo, M. Zobov, Bunch length control in DAΦNE by a higher harmonic cavity. Nucl. Instrum. Methods Phys. Res. Sect. A **354**(2–3), 215–223 (1995). https://doi.org/10.1016/0168-9002(94)01005-6
12. T. Phimsen, B.C. Jiang, H.T. Hou et al., Improving Touschek lifetime and synchrotron frequency spread by passive harmonic cavity in the storage ring of SSRF. Nuc. Sci. Tech. **28**, 108 (2017). https://doi.org/10.1007/s41365-017-0259-y
13. R. Biscardi, S.L. Kramer, G. Ramirez, Bunch length control in the NSLS VUV ring. Nucl. Instrum. Methods Phys. Res. Sect. A **366**(1), 26–30 (1995). https://doi.org/10.1016/0168-9002(95)00522-6
14. R.A. Bosch, C.S. Hsue, Suppression of longitudinal coupled-bunch instabilities by a passive higher harmonic cavity, in *Particle Accelerator Conference, 1993, Proceedings of the 1993* (IEEE, 1993), pp. 3369–3371. https://doi.org/10.1109/pac.1993.309653
15. J.M. Byrd, M. Georgsson, Lifetime increase using passive harmonic cavities in synchrotron light sources. Phys. Rev. Spec. Top. Accel. Beams **4**(3), 030701 (2001). https://doi.org/10.1103/PhysRevSTAB.4.030701
16. M. Borland, elegant: A flexible SDDS-compliant code for accelerator simulation (Argonne National Lab, Lemont, 2000). https://doi.org/10.2172/761286
17. A. Xiao, V. Sajaev, Simulation study of injection performance for the advanced photon source upgrade, in *Proceedings of IPAC2015, Richmond, VA, USA* (2015), pp. 1816–1818. https://doi.org/10.18429/jacow-ipac2015-tupje075
18. A. Xiao, M. Borland, C. Yao, On-axis injection scheme for ultra-low-emittance light sources, in *WEPSM13, Proceedings of PAC2013, Pasadena, CA USA*